Piezospectroscopic coatings: Effects of alumina nanoparticle volume fraction on stress-sensing

Remelisa Esteves, Ryan Hoover, Khanh Vo, and Seetha Raghavan
University of Central Florida
4000 Central Florida Boulevard
Orlando, FL 32816

ABSTRACT

Coatings with embedded photo-luminescent alumina nanoparticles as "sensors" have shown potential for detecting signs of damage within the underlying substrates. Chromium-doped alumina is naturally photo-luminescent with spectral properties that are characterized by two distinct peaks known as R-lines. When the material is subjected to stress, shifts in the R-lines occur, which is known as the piezospectroscopic effect. Recent work has shown that improved sensitivity of the technique can be achieved through a configuration of nanoparticles within a polymer matrix, which can be applied to a structure as a stress-sensing coating. This study demonstrates the capability of piezospectroscopic coatings in mechanical tests and investigates the effect of nanoparticle volume fraction on sensing performance. Here, we show measurements of spectral shifts that capture variation in stress of the coating during a mechanical test and in the region of substrate damage. The results show the ability to design and tailor the "sensing" capability of these nanoparticles and correlate the measured stress variations with the presence of stress and damage in underlying structures. This study is relevant to nondestructive evaluation in the aerospace industry, where monitoring signs of damage is of significance for testing of new materials, quality control in manufacturing and inspections during maintenance.

1. INTRODUCTION

The aerospace industry relies on nondestructive evaluation (NDE) methods to determine material properties of new materials through standardized tests and quality inspection during manufacturing and maintenance [1]. One of the significant concerns is monitoring the health of aerospace structures. Metallic components tend to age due to some major flaws, including fatigue damage, hidden cracks and corrosion [2]. Recently, there has been an increasing trend of the use of composite materials in aerospace structures. Composite materials are well known for having high strength-to-weight ratios and corrosion resistance; thus making them advantageous over metallic materials. Structures made from composite materials may fail due to delamination, matrix crack, fiber-matrix debonding and fiber breakage [3]. Failure prediction and detection is critical for aircraft structural integrity. NDE methods must be sensitive enough to detect these flaws and provide reliable results [4]. Due to the increasing interest in structural health monitoring [5], the aerospace industry seeks new and improved NDE methods. In this study, the sensitivity of a stress-sensing nanoparticle coating concept, using piezospectroscopy, is investigated specifically for the effect of nanoparticle volume fraction on sensing performance.

Photo-luminescence spectroscopy of chromium-doped alpha-alumina, a naturally photo-luminescent material, characterizes two distinct peaks R1 and R2, from the material, called R-lines [6] shown in Figure 1. Intensities of R-lines have been used in our previous work to study dispersion of alumina nanoparticles in hybrid carbon fiber reinforced polymers (HCFRPs). HCFRPs utilize nanoparticles of alpha-alumina embedded into carbon fiber reinforced polymers

to improve fracture toughness properties [7]. While embedding nanoparticles into carbon fiber enhances mechanical properties, achieving uniform dispersion is a challenge since agglomerations and sedimentation can occur [7]. Dispersion studies using photo-luminscence spectroscopy enables the identification of regions of increased agglomeration [8] and demonstrates capability of characterizing particle dispersion [9] for applications in assessing manufacturing quality.

Piezospectroscopy (PS) correlates changes in the peak position of laser-induced spectral emission of photo-luminescent materials when they undergo stress. Historically, this method has been used to measure the amount of pressure in diamond-anvil cells [8]. It is also applicable to structural health monitoring of thermal barrier coatings (TBCs) in turbine engines [10, 11]. Through photo-luminescence piezospectroscopy, the stress state of TBCs can be analyzed from the thermally grown oxide (TGO), which is a chromium-doped α-alumina layer [12]. The fundamental method is demonstrated when stress is applied to the material, where a shift in the R-lines can be observed. This phenomenon is known as the piezospectroscopic effect and can be expressed in the relationship shown in Equation 1 [13].

$$\Delta\nu=\pi_{ij}\sigma_{ij} \quad [1]$$

Here π_{ij} represents the piezospectroscopic coefficients, and $\Delta\nu$ represents the change in wavenumber from the peak shift while σ_{ij} is the stress tensor.

Our work focuses on the investigation of a stress-sensing material based on the piezospectroscopic effect and comprises a polymer matrix with embedded α-alumina nanoparticles which can be applied on a substrate. Here, the nanoparticles can be configured to improve the sensitivity of the measurements. In our previous study on the effect of nanoparticle volume fraction on stress sensing, mechanical tests were performed on epoxy material with variations in volume fractions of nanoparticles. It was determined that the stress-sensitivity, represented by the slope of the peak shift against the applied stress, increased as the volume fraction of nanoparticles increased [14, 15].

When implementing this material consisting of epoxy and alumina nanoparticles as a piezospectroscopic coating for the study of aerospace materials, the ability to sense stress variations when the materials are subjected to loading has been successfully demonstrated. In the study by Freihofer et al [16], an open-hole tension (OHT) carbon fiber reinforced polymer (CFRP) was coated with epoxy that consisted of 20 % volume fraction of alumina nanoparticles and tested in accordance with ASTM D5766 [17]. It was found that the coating detected signs of internal ply damage at 77 % failure load [16] well before it surfaced and was visually detected at 92 % of the failure load.

The current study presented here demonstrates the sensitivity of stress and damage detection with piezospectroscopic (PS) coatings as a function of the volume fraction of nanoparticles within the coating. The study is an initial effort to answer the need to define optimal parameters for an ideal working configuration of this piezospectropic coating in order to enable the implementation and technique to complement other NDE methods that are currently being used, such as ultrasonic and eddy current. Here, spectral data from the three samples with 5 % and 10 % volume fraction of alumina within a PS coating on hard laminate and 20 % volume fraction of

alumina on soft laminate tested in a previous study [16] are compared for their sensitivity in stress and damage detection. In addition, two of the damaged OHT CFRP test specimens were assessed for post damage investigation using the piezospectroscopic coating.

2. EXPERIMENTATION & ANALYSIS

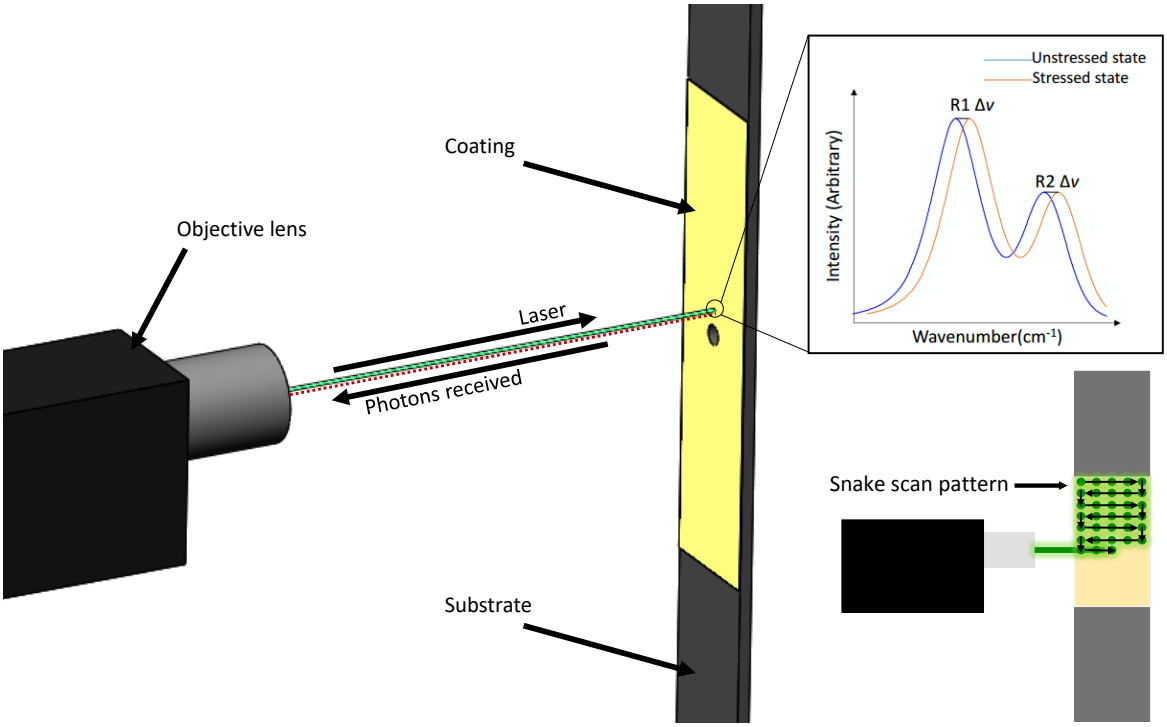

Figure 1. A schematic showing PS data collection

2.1 Mechanical Loading tests

The PS nanocoating investigated was manufactured by Elantas PDG Inc. by mixing 150 nm α-Al_2O_3 nanoparticles (Inframat Corp.) with 99.8 % purity in epoxy to achieve 5 %, 10 % and 20 % volume fraction of particles. The coating was applied to an open-hole tension composite substrate consisting of laminated IM7-8552 unidirectional tape. Two OHT CFRP hard laminate specimens were coated with 5 % and 10 % volume fraction PS coatings. These composite substrates had an elastic modulus of 91 GPa. An OHT CFRP soft laminate specimen was coated with 20 % volume fraction PS coating. This composite substrate had an elastic modulus of about 38.6 GPa. The laminates and corresponding coating configurations are shown in Table 1. Each specimen was loaded at a rate of 0.02 mm/sec, held at discrete increments using displacement control and loaded until failure. The hard laminate specimens were loaded up to 88,964 N, while the soft laminate specimen was loaded up to 44,482 N. PS data were collected using a 60 x 60 grid in a snake scan pattern, a measurement area of 25.4 square mm, and a spatial resolution of 0.4 mm. The portable photo-luminescent piezospectroscopy system collects data in a snake scan pattern by taking point scans of a defined area on the sample with a laser probe. This is shown in Figure 1. The system continues this pattern until it scans the entire defined area. The maps were collected within 8 minutes for the sample with 20 % volume fraction of alumina [19]; within 14 minutes for the sample with 10 % volume fraction of alumina; and within 32 minutes for the

sample with 5 % volume fraction of alumina to gain sufficient intensity with respect to the amount of particles in the coating. More information on the snake scan pattern and experimental setup is available in previous publications [14, 16].

2.2 Spectral Analysis

The analysis of this data was conducted using a set of in-house, non-linear, least squares codes that allow for the processing of large data sets in a relatively short amount of processing time. This consists of a set of curve-fitting algorithms that process the unique R-line doublet that makes up the photo-luminescent response of alumina using two pseudo-Voigt functions. The details of curve fitting of experimental data using two pseudo-Voigt functions are further described in a previous publication [18].

3. RESULTS

The sensing capability of the three coating configurations is analyzed in this section. These PS coatings consist of 5 %, 10 % and 20 % volume fraction of alumina. The 5 % and 10 % volume fraction PS coatings were applied to the composite substrates with hard laminate, while the 20 % volume fraction PS coating was applied to the composite substrate with soft laminate. First, the strength of the signal response coming from the PS coatings was determined based on the representative R-lines and average signal-to-noise ratios (SNR). Then, comparisons of the peak shift maps during the course of the tensile tests for each OHT CFRP sample were made to determine differences in damage sensing capability on the hard laminate and the soft laminate. Lastly, the dispersion and peak shift maps of the samples with 5 % and 10 % volume fraction PS coatings after damage had taken place were analyzed.

3.1 R-lines of PS Coatings

To verify the signal response coming from the PS coatings, the representative R-lines for each coating configuration were analyzed, as shown in Figure 2. The average SNR value and average coating luminosity value for each coating configuration and corresponding to the representative R-lines in Figure 2 are listed in Table 1. The average SNR values were taken from the average of all SNR values correlating with one peak shift contour map, which consists of R-lines from 3600 point locations. The average coating luminosity values were determined by taking the average intensity values correlating with one peak shift contour map divided by the collection time. For consistency, the same x-y coordinates were used to pick a particular point on each map to display the R-lines.

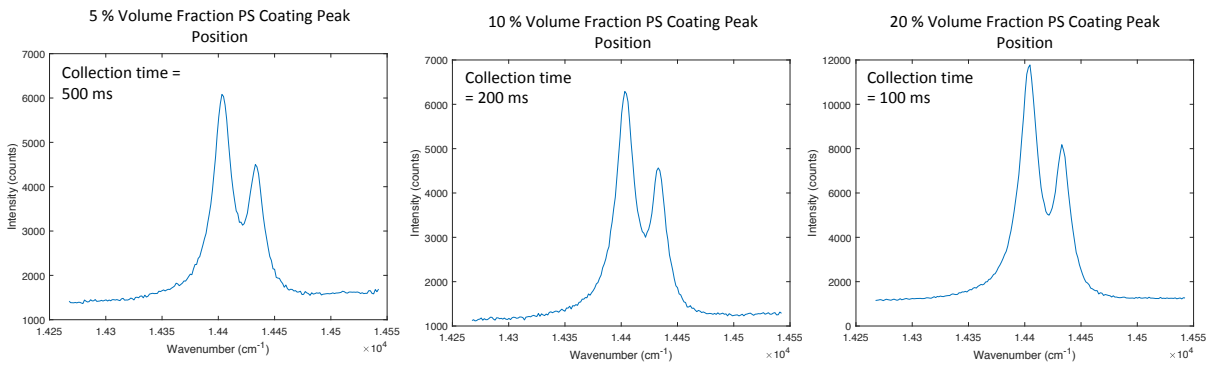

Figure 2. Representative R-lines for each PS coating with corresponding collection times. Laser power and beam diameter was kept consistent for each sample.

Table 1. SNR values for each PS coating

Laminate Type	PS Coating Volume Fraction	Average SNR Value	Average Coating Luminosity
Hard	5 %	43.35	8,371 counts/sec
Hard	10 %	58.36	25,263 counts/sec
Soft	20 %	95.92	106,103 counts/sec

The R-lines indicate that signal was received from those points, and they show intensity with respect to collection time. The average SNR values measure the quality of the R-lines for each PS coating configuration. These values are further supported by the average coating luminosity values. The higher the average SNR and average coating luminosity values, the lesser the uncertainty in the peak position and the smoother the R-lines. For OHT CFRP specimens with hard laminate, the 10 % volume fraction PS coating had higher average SNR value and average coating luminosity value than that of the 5 % volume fraction PS coating despite shorter collection times. The 5 % volume fraction PS coating can potentially achieve the same average SNR value as the 10 % volume fraction PS coating or higher, but it would take a longer time to achieve that value. This comparison of average SNR values shows that the 10 % volume fraction PS coating should have lesser uncertainty in the peak position, and thus show more discernable peak shifts, compared to the 5 % volume fraction PS coating. The 20 % volume fraction PS coating with soft laminate had the highest average SNR value of 95.92 in comparison with the 5 % and 10 % volume fraction PS coatings. It achieves this average SNR value at a collection time of 100 ms, which is the shortest time among the other coating configurations. Based on these observations, higher average SNR and average coating luminosity correlate with more distinctive peak shifts.

3.2 Peak Shift Maps for PS Coatings of Varying Volume Fractions

Peak shift maps for the 5 % and 10 % volume fraction PS coatings were compared to observe differences in stress sensing capability on hard laminate, as shown in Figure 3.

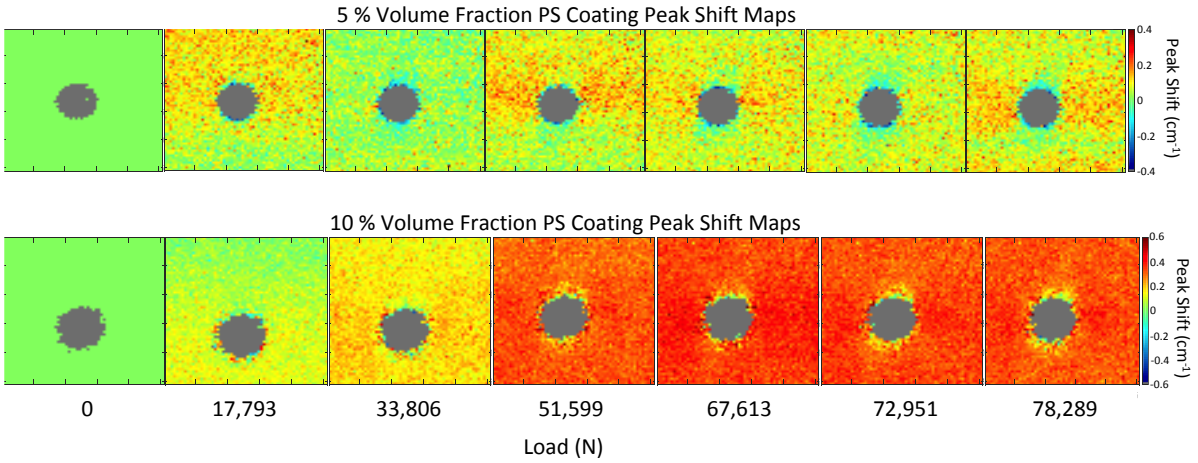

Figure 3. Stress sensing of the OHT CFRP specimens with 5 % (top) and 10 % (bottom) volume fraction PS coatings with progressing loads. Both specimens consist of composite substrates with hard laminate. Each map has dimensions of 25.4 mm × 25.4 mm.

These maps show peak shifts based on the type of stress that the specimens were experiencing. A positive shift indicates tensile stress, while a negative shift indicates compressive stress. The PS maps for both hard laminate specimens show strain release around the hole with increasing load. However, due to the high elastic modulus of this hard laminate substrate, there is not a significant change in the strain release compared to the soft laminate presented in the following section. Starting at 51,599 N, signs of tensile loading is clearly shown on the PS map for the 10 % volume fraction PS coating. On the other hand, at the same load, the PS map for the 5 % volume fraction PS coating showed only a slight change in stress. Based on this comparison, the 10 % volume fraction PS coating shows more sensitivity to changes in stress than the 5 % volume fraction PS coating. The higher average SNR value for the 10 % volume fraction PS coating than for the 5 % volume fraction PS coating shown in Table 1 is likely to have contributed to this.

The peak shift maps for the 20 % volume fraction PS coating was observed for the coating's stress sensing capability on soft laminate, as shown in Figure 4.

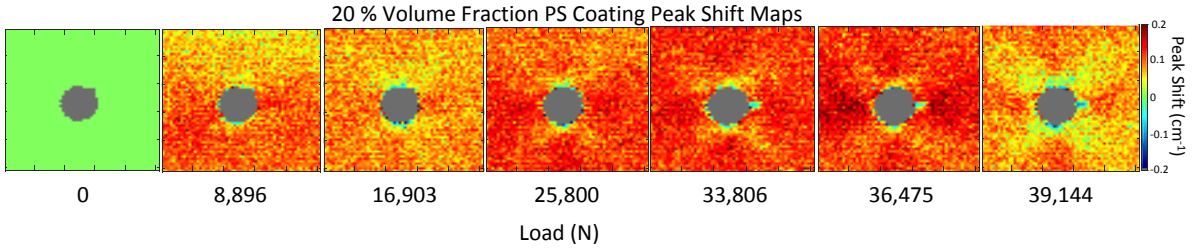

Figure 4. Stress sensing of OHT CFRP specimen with 20 % volume fraction PS coating. This specimen consists of composite substrates with soft laminate. Each map has dimensions of 25.4 mm × 25.4 mm.

Intrinsic stress patterns are shown in the maps with progressive loading. Starting at 33,806 N, initiation of damage adjacent to the open hole can be observed. This region was experiencing large tensile strains and was a likely location for damage to initiate [19]. Work by Camanho [20] supports this phenomenon in which he performed a simulation using continuum damage mechanics of a transversely isotropic open hole tension composite specimen and predicted initial fiber failure in the 0° ply in the same region. At 39,144 N, the PS map shows a more distinct variation of stresses within the sample, which is likely caused by progressive damage and subsequent redistribution of stresses [19]. Significant variation of stresses on soft laminate is distinctly shown in the PS maps, which indicates that the PS coating can easily sense the changes in stress on this type of laminate. Specifically, the elastic modulus of the soft laminate is lower than that for the hard laminate, which means that the soft laminate is more susceptible to large stresses at lower applied loads compared to the hard laminate. Due to the changes in stress that the soft laminate experiences, distinct stress patterns can be clearly seen in maps of Figure 4 at high applied loads. The high stress-sensitivity of this 20 % volume fraction PS coating can also be attributed to the high average SNR value (Table 1). The strong signal coming from the alumina nanoparticles results in distinct peaks that produce more discernible peak shifts.

3.3 Dispersion and Peak Shift Maps for 5 % and 10 % Volume Fraction PS Coatings after damage

Map scans of the OHT CFRP samples with 5 % and 10 % volume fraction of alumina were taken after damaged was induced on them. Figure 5 shows the dispersion and peak shift maps that demonstrate the aftermath of the tensile tests. Coatings for these samples were visually inspected and showed no signs of coating delamination around the hole where the sample was intact.

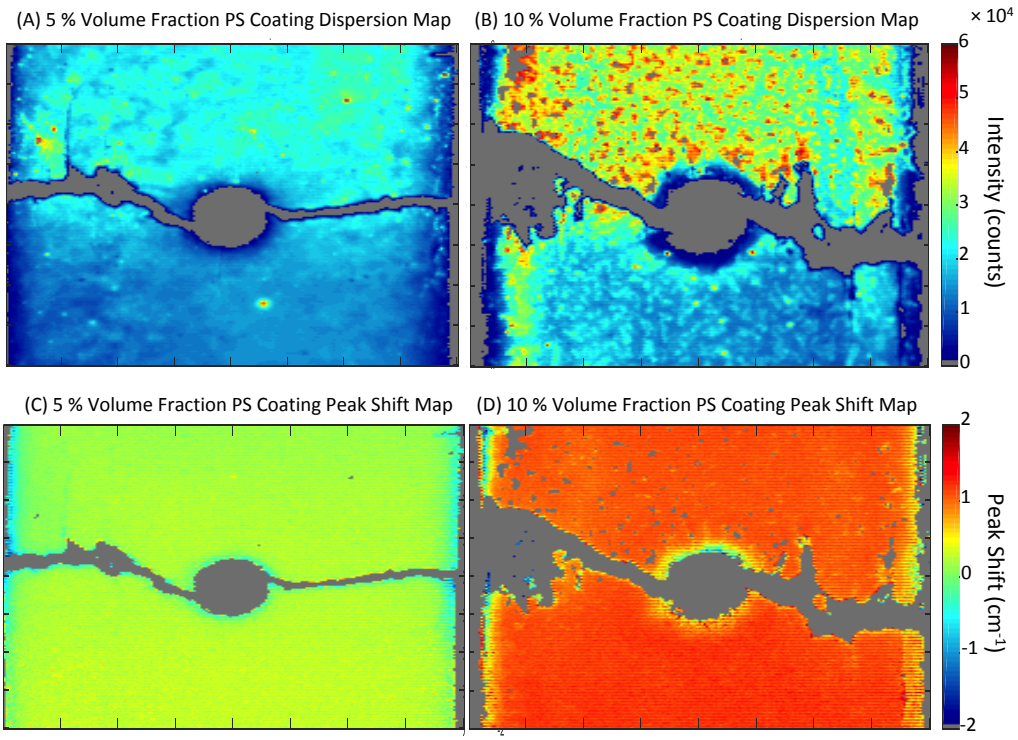

Figure 5. Contour maps of the OHT CFRP samples showing (A) particle dispersion for 5 % volume fraction PS coating, (B) particle dispersion for 10 % volume fraction PS coating, (C) peak shift for 5 % volume fraction coating, and (D) peak shift for 10 % volume fraction coating. Each map has dimensions of 40 mm × 40 mm.

The intensities of the photoluminescence in the coating demonstrate the overall dispersion of the coating during manufacturing. From the dispersion maps in Figure 5 it is seen that the 5 % volume fraction PS coating had fairly uniform distribution of alumina particles overall, whereas the 10 % volume fraction PS coating had some agglomeration of particles at the top region of the sample. The peak shift maps for both coatings, however, show mostly uniform residual stress after damage in the unloaded condition. Therefore, it is observed that small amounts of dispersion variation do not affect the coating sensing.

The peak shift maps from Figure 3 indicate a changing stress state around the hole for all three samples. The peak shift maps of Figure 5 in the post-damage condition indicate that this relaxed stress state around the hole is retained, representing that permanent deformation has occurred in the composite in this location. The 10 % volume fraction coating shows this more prominently. Both 5 % and 10 % volume fraction coatings shown here are therefore capable of detecting post-damage permanent deformation.

4. CONCLUSIONS

The demonstration that the sensing capability of the PS coatings can be designed and tailored was achieved in this study. Notable differences in capturing the stress variations that will correlate with the presence of crack initiation and propagation in each OHT CFRP specimen

were observed in the PS maps. For the hard laminate specimens, the 10 % volume fraction PS coating showed more sensitivity in sensing stress based on the PS maps and SNR values when comparing the 5 % and 10 % volume fraction PS coatings. Comparing the PS maps for the hard laminate and the soft laminate, it is evident that, within the range of volume fractions tested, differences in stress are more clearly defined for the PS coating on soft laminates with lower applied loads. This is because the soft laminate has a smaller elastic modulus in comparison with the hard laminate's elastic modulus. Thus, the changes in stress show more distinctly on the PS maps. This is amplified by the fact that the 20 % volume fraction coating has the highest average SNR value with a strong signal coming from the alumina nanoparticles resulting in more distinct shifts. For the ranges of PS coating volume fractions and both the hard and soft laminates that were tested, the dispersion of the alumina nanoparticles does not affect the sensitivity in stress sensing. Current work is focused on optimizing luminescence efficiency. Specifically, the aim is to improve on the optics technology to achieve faster scan time and larger scan area and the materials technology to improve PS sensing. Future work will focus on investigating coating degradation under various environmental conditions.

5. ACKNOWLEDGEMENTS

Dr. Gregory Freihofer is acknowledged for his efforts on developing the piezospectroscopic coating configurations, conducting the mechanical test experiments and providing the data used in this work. The Boeing Company is acknowledged for their assistance with Dr. Freihofer's experiments. This work was supported by the National Science Foundation under Grant Nos. IIP 1701983 and CMMI 1130837.

6. REFERENCES

1. UnnÞòrsson, R., Jonsson, M. T., & Runarsson, T. P. (2004). NDT methods for evaluating carbon fiber composites. *Proceedings of the Composites Testing and Model Identification, Bristol, UK*, 21-23.
2. Giurgiutiu, V., Redmond, J. M., Roach, D. P., & Rackow, K. (2000, March). Active sensors for health monitoring of aging aerospace structures. In *PROCEEDINGS-SPIE THE INTERNATIONAL SOCIETY FOR OPTICAL ENGINEERING*(pp. 294-305). International Society for Optical Engineering; 1999.
3. Ghobadi, A. (2017). Common Type of Damages in Composites and Their Inspections. *World Journal of Mechanics*, *7*(02), 24.
4. Riegert, G., Pfleiderer, K., Gerhard, H., Solodov, I., & Busse, G. (2006). Modern methods of NDT for inspection of aerospace structures. *ECNDT, Berlin, Germany*.
5. Farrar, C. R., & Worden, K. (2007). An introduction to structural health monitoring. *Philosophical Transactions of the Royal Society of London A: Mathematical, Physical and Engineering Sciences*, *365*(1851), 303-315.
6. Stevenson, A., Jones, A., & Raghavan, S. (2011). Characterization of particle dispersion and volume fraction in alumina-filled epoxy nanocomposites using photo-stimulated luminescence spectroscopy. *Polymer journal*, *43*(11), 923-929.

7. Hanhan, I., Selimov, A., Carolan, D., Taylor, A. C., & Raghavan, S. (2017). Quantifying Alumina Nanoparticle Dispersion in Hybrid Carbon Fiber Composites Using Photoluminescent Spectroscopy. *Applied Spectroscopy*, *71*(2), 258-266.
8. Hanhan, I. (2015). Hybrid Carbon Fiber Alumina Nanocomposite for Non-Contact Stress Sensing Via Piezospectroscopy.
9. Selimov, A., Hoover, R., Fouliard, Q., Manero II, A., Dackus, P., Carolan, D., ... & Raghavan, S. (2017). Characterization of Hybrid Carbon Fiber Composites using Photoluminescence Spectroscopy. In *58th AIAA/ASCE/AHS/ASC Structures, Structural Dynamics, and Materials Conference* (p. 0123).
10. Clarke, D. R., Oechsner, M., & Padture, N. P. (2012). Thermal-barrier coatings for more efficient gas-turbine engines. *MRS bulletin*, *37*(10), 891-898.
11. Majewski, M. S., Kelley, C., Lake, J., Renfro, M. W., Hassan, W., Brindley, W., & Jordan, E. H. (2012). Stress measurements via photoluminescence piezospectroscopy on engine run thermal barrier coatings. *Surface and Coatings Technology*, *206*(11), 2751-2758.
12. Heeg, B., & Clarke, D. R. (2005). Non-destructive thermal barrier coating (TBC) damage assessment using laser-induced luminescence and infrared radiometry. *Surface and Coatings Technology*, *200*(5), 1298-1302.
13. Hanhan, I., Durnberg, E., Freihofer, G., Akin, P., & Raghavan, S. (2014). Portable Piezospectroscopy system: non-contact in-situ stress sensing through high resolution photo-luminescent mapping. *Journal of Instrumentation*, *9*(11), P11005.
14. Stevenson, A., Jones, A., & Raghavan, S. (2011). Stress-sensing nanomaterial calibrated with photostimulated luminescence emission. *Nano letters*, *11*(8), 3274-3278.
15. Stevenson, A. L. (2011). *Calibration of alumina-epoxy nanocomposites using piezospectroscopy for the development of stress-sensing adhesives* (Doctoral dissertation, University of Central Florida).
16. Freihofer, G., Dustin, J., Tat, H., Schülzgen, A., & Raghavan, S. (2015). Stress and structural damage sensing piezospectroscopic coatings validated with digital image correlation. *AIP Advances*, *5*(3), 037139.
17. ASTM Standard D5766/D5766M-11, 2011, "Standard Test Method for Open-Hole Tensile Strength of Polymer Matrix Composite Laminates" ASTM International, West Conshohocken, PA, 2011, DOI: 10.1520/D5766_D5766M-11, www.astm.org.
18. Freihofer, G. (2014). Nanocomposite coating mechanics via piezospectroscopy. Ph. D. Dissertation submitted to the University of Central Florida.
19. Freihofer, G., Schülzgen, A., & Raghavan, S. (2015). Damage mapping with a degrading elastic modulus using piezospectroscopic coatings. *NDT & E International*, *75*, 65-71.
20. Camanho, P. P., Maimí, P., & Dávila, C. G. (2007). Prediction of size effects in notched laminates using continuum damage mechanics. *Composites science and technology*, *67*(13), 2715-2727.